

Current correlations of an on-demand single-electron emitter

A. Mahé,¹ F. D. Parmentier,¹ E. Bocquillon,¹ J.-M. Berroir,¹ D. C. Glatthli,^{1,*} T. Kontos,¹ B. Plaçais,¹ G. Fève,^{1,†} A. Cavanna,² and Y. Jin²

¹Laboratoire Pierre Aigrain, Ecole Normale Supérieure, CNRS (UMR 8551), Université P. et M. Curie–Université D. Diderot, 24, rue Lhomond, 75231 Paris Cedex 05, France

²Laboratoire de Photonique et Nanostructures, Marcoussis, France

(Received 22 October 2010; published 12 November 2010)

In analogy with quantum optics, short-time correlations of the current fluctuations are measured and used to assess the quality of the single-particle emission of a recently introduced on-demand electron source. We observe, in the context of electronics, the fundamental noise limit associated with the quantum fluctuations of the emission time of single particles, or quantum jittering. In optimum operating conditions of the source, the noise reduces to the quantum jitter limit, which demonstrates single-particle emission. Combined with the coherent manipulations of single electrons in a quantum conductor, this electron quantum optics experiment opens the way to explore new problems including quantum statistics and interactions at the single-electron level.

DOI: [10.1103/PhysRevB.82.201309](https://doi.org/10.1103/PhysRevB.82.201309)

PACS number(s): 73.23.Ad, 73.43.Fj, 72.70.+m

Coherent ballistic electronic transport bears strong analogies with the propagation of photons. In particular, the edge states of a two-dimensional electron gas in the quantum-Hall regime form a promising realization of one-dimensional ballistic quantum rails. In this system, electronic interferences have been observed in Mach-Zehnder interferometers,¹ using continuous electron sources based on voltage-biased contacts. The electronic analog of quantum optic experiments,^{2,3} based on the ultimate control and manipulation of single electrons in quantum conductors, could be implemented using the recently proposed single-electron emitters^{4,5} combined with the development of current correlation measurements on single-electron beams. Furthermore, these “electron quantum optic” experiments bear also strong differences with their photonic counterpart. Electron and photon statistics differ, and a great richness is also brought by the presence of Coulomb interaction inducing relaxation⁶ and decoherence⁷ of electronic excitations. In this respect, single-electron emitters offer a route to study the complex many-body interaction of a single excitation propagating in the presence of a Fermi sea.⁸ Some fundamental questions already arise when one wants to study the elementary processes involved in the transfer of a single charge from a dot to a one-dimensional lead.^{9,10} First, the number of transferred charges can fluctuate (0, 1, or 2) if the emitter is not perfect. Another process, specific to the electronic case, involves the collateral emission of spurious electron/hole pairs.^{10,11} It is known from optics that only the short-time intensity-intensity correlations of light $\langle I(t)I(t+t') \rangle$ can ensure on-demand emission of a single photon. For perfect single-particle emission, if a particle is detected at time t [$I(t) \neq 0$], no other particle is detected at time $t+t' \neq t$ and $\langle I(t)I(t+t') \rangle \propto \delta(t')$. This so-called Hanbury-Brown and Twiss (HBT) interferometry has attracted wide interest in the characterization of a large variety of single photon emitters.¹² In the context of on-demand electron emitters, these techniques could demonstrate the realization of a “clean” emission process resulting in the emission of a single electronic excitation above the Fermi sea of the lead at each trigger of the source.

In this Rapid Communication, we report on the HBT short-time correlations measurements of a periodically

driven on-demand electron source with subnanosecond time control.⁴ In Ref. 4, the phase-resolved measurement of a quantized ac current in multiples of $2ef_d$, where f_d is the drive frequency, has brought evidence that the source emits, on average, one electron followed by one hole at each period of the excitation signal. Here a breakthrough is reached by the measurement of the short-time autocorrelation (or high-frequency noise) of the current emitted by this electron source. We demonstrate the existence of two noise limits. The first one is the standard shot noise associated with the fluctuation of the charge emitted by the source at each period of the drive. The second one is a different electronic noise, showing up at high frequency and caused by the quantum uncertainty in the tunneling escape time of electrons, which we therefore call quantum jitter. This jitter or phase noise, is the direct analog of the one observed for triggered single-photon sources.¹² In optimum operating conditions of the source, shot noise disappears and the current fluctuations reduce to the quantum jitter, demonstrating that exactly one single particle is emitted at each half period of the excitation signal. This quantum jitter limit is thus the hallmark of a perfect triggered single-particle emitter. Low-frequency shot-noise suppression has already been observed in pumps. However, the time resolution was not sufficient to reveal the quantum jitter.¹³

The source is made of a submicronic quantum dot [see Fig. 1(a)] coupled to a two-dimensional electron gas (2DEG) by a quantum point contact (QPC), used as a tunnel barrier of tunable transmission. We work at a high magnetic field, $B \approx 1.8$ T, in the quantum-Hall regime with a filling factor $\nu=4$ in the 2DEG leads. The QPC gate voltage V_g is set to control the transmission D of the outermost edge state between the dot and the electron gas while inner edge states are reflected. By capacitive coupling, V_g also controls the static potential of the dot and shifts the position of the dot discrete spectrum with respect to the Fermi energy. The dot is also capacitively coupled to a metallic top-gate connected to a high-frequency broadband coaxial line. A square ac voltage $V_{exc}(t)$ (of peak to peak amplitude $2V_{exc}$) can thus control the dot potential on subnanosecond time scales with a 20–80 % rise time of 60 ps. The dot-level spacing $\Delta=4.2$ K is respon-

sible for a finite-energy cost for the addition of a single charge inside the dot (the dot Coulomb energy was found negligible in Ref. 4, probably due to the large top gate and is neglected throughout this Rapid Communication). The emission of electrons is triggered by the sudden rise ($2eV_{exc} \approx \Delta$) of the dot potential which brings the last occupied energy level of the quantum dot [see scheme in Fig. 1(b)] above the Fermi energy. It is expected that a single charge is emitted on an average escape time $\tau = h/\Delta \times (1/D - 1/2) \approx h/D\Delta$ for $D \ll 1$.⁴ By resetting the potential to its initial value, the dot is reloaded by the absorption of one electron in the average time τ , leaving a hole emitted in the Fermi sea. Repeating this sequence at frequency $f_d = 1.5$ GHz, the periodic emission (with period $T = 1/f_d$) of a single electron followed by a single hole can be achieved. The charges emitted by the dot are collected in a 120Ω resistor connected to an rf transmission line allowing for the measurement of the average current and the current noise spectrum emitted by the dot. As observed in Refs. 4 and 14, the average current reproduces the exponential time relaxation on a characteristic time $\tau = RC$ of a classical RC circuit driven by a square excitation of amplitude $2V_{exc} = C/e$: $\langle I(t) \rangle = \frac{e}{\tau} \frac{e^{-t/\tau}}{1 + e^{-T/2\tau}}$ (for $0 \leq t \leq T/2$). For short escape times $\tau \ll T/2$, the average emitted charge per half period is quantized: $Q = \int_0^{T/2} dt \langle I(t) \rangle = e$. For escape times comparable to or larger than the half period $\tau \geq T/2$, electrons do not have enough time to escape which results in a nonunit emission probability $P < 1$ so that $Q = P \cdot e < e$ with $P = \tanh(T/4\tau)$. In the frequency domain, quantization of the emitted charge shows up in a quantization of the modulus of the first harmonic of the current $|I_{f_d}| = 2ef_d$ which can be observed in Fig. 1(c) representing a color plot of $|I_{f_d}|$ as a function of the excitation amplitude and QPC gate voltage. White diamonds can be seen where $|I_{f_d}| = 2ef_d$. These diamonds disappear at small transmission for $\tau \geq T/2$, ($P < 1$), and are blurred at large transmission $D \approx 1$ because of quantum fluctuations of the dot charge.

Although the observation of current quantization is a strong indication that single charge emission is achieved, the quality of the source can be ascertained by the measurement of the current noise spectrum. In particular, only the latter rules out spurious multiple particle emission. This is the purpose of this Rapid Communication, where we focus on high-frequency noise measurements for an excitation amplitude matching the level spacing, $2eV_{exc} = \Delta$ corresponding to the red dashed line in Fig. 1(c).

Measurements of the high-frequency fluctuations of the electron source differ completely from usual noise measurements in steady-state situations either at low¹⁵ or high frequency.¹⁶ First, as the circuit is periodically driven, the statistical average of current fluctuations $C(t, t') = \langle \delta I(t) \delta I(t + t') \rangle$ depends as usual on the time difference t' but also periodically on the absolute time t . We will focus in this Rapid Communication on the current correlations averaged, not only on a statistical ensemble, but also on time t , $C(t') = \langle \delta I(t) \delta I(t + t') \rangle^t$, and on the noise spectrum $S(\omega) = 2 \int dt' C(t') e^{i\omega t'}$. Second, the intrinsic ac coupling of the circuit blocks dc current and the current noise spectrum vanishes at zero frequency $S(\omega = 0) = 0$. We have measured the noise power in the 1.2–1.8 GHz band centered on the drive

frequency $f_d = 1.5$ GHz, excluding the drive frequency using notch filters. Using an absolute calibration with a thermal source of variable temperature, we obtain accurate measurements of $S(\omega \approx 2\pi f_d)$.

To analyze our experimental results presented in Fig. 2, we first extract Q and τ from the modulus and phase of the current first harmonic, considering the exponential dependence of the average current in time domain. Q and τ have been plotted in Fig. 2(a) as a function of V_g . As the average escape time τ rises from 20 ps ($\approx T/30$) to a few nanoseconds ($\approx 2T$), the emitted charge decreases from a quantized value e ($P = 1$) when $\tau \ll T/2$ to $P \cdot e$ ($P \ll 1$) when $\tau \gg T/2$. As can be seen in Fig. 2(a), the $P(\tau)$ dependence is very well accounted for by $P = \tanh(T/4\tau)$ (black dashed line). Having characterized the probability to emit one charge per half period, we can make a simplified estimation of the current noise by analogy with low-frequency partition noise where P would be the partitioning probability. In this case, the low-frequency current spectrum S is fully characterized by P , $S = 2e \times 2ef_d \times P(1 - P)$ going from shot noise for $P \ll 1$ to shot-noise suppression for $P = 1$. In accordance with our simple expectation, $S(2\pi f_d)$ presented in Fig. 2(b) as a function of V_g scales in units of $e^2 f_d$. It vanishes for $D \approx 0$, ($P \ll 1$) and reaches a maximum for $P \approx 1/2$. However, in the $Q = e$ regime ($V_g \gtrsim -0.3425$ V), we still measure a large noise which cannot be interpreted by standard shot noise which is suppressed by the $(1 - P)$ factor.¹⁵ $S(2\pi f_d)$ can even approach its maximum value in this domain. In addition, $S(2\pi f_d)$ exhibits oscillations as function of V_g which minima coincide with the center of the diamonds of Fig. 1(c) and maxima with their edges.

To understand the experimental results, we rely on a toy model of the electron source. The period T of the excitation signal is divided in units of τ_0 , the time needed for electrons to make one round trip inside the dot. When promoted above the chemical potential during the first half period of the drive, the electron attempts to escape with probability b every τ_0 . If it escapes, no additional electron is allowed to escape and a hole can be emitted during the next half period following the same rules. If the electron does not escape, the emission of the hole is forbidden. The average current computed in this model reproduces the exponential decay on a time $\tau = \tau_0 \times (1/b - 1/2)$ with an averaged emitted charge per half period $Q = P \cdot e$, $P = \tanh[T/4\tau(b)]$. The two contributions $C_1(t') = \overline{\langle I(t) I(t + t') \rangle}^t$ and $C_2(t') = \overline{\langle I(t) \rangle \langle I(t + t') \rangle}^t$ to the current fluctuations $C = C_1 - C_2$ calculated using the toy model have been plotted in Fig. 3(a) in the case of unit emission probability $P \approx 1$ ($b = 0.2$). C_2 is the product of the statistical averages of the current, it reproduces alternating peaks centered on electron and hole triggers ($t' = n \times T/2$) and of typical width given by the average escape time τ . For times $t' \geq T/2$, C_1 equals C_2 reflecting the absence of correlations between two successive electron/hole emissions. However, on short times $t' < T/2$, C_1 differs strongly from C_2 : $C_1(t') \propto \delta(t')$ is a Dirac peak proportional to P . As stated before, this is the hallmark of a single-particle emitter: the emission of an electron cannot be followed by that of another one. This result can be extended beyond this toy model. In full generality, considering the emission of a single particle

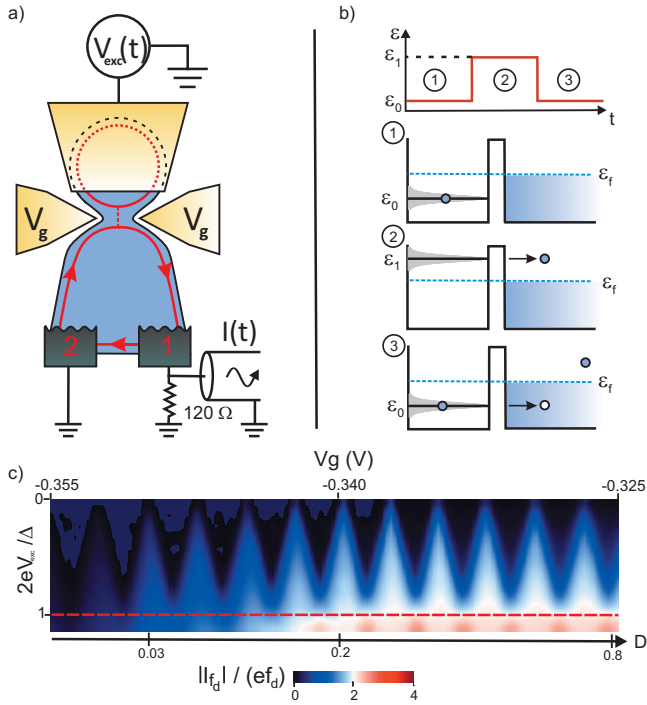


FIG. 1. (Color) (a) Sketch of the circuit. A single edge state is transmitted between the dot and the leads with transmission probability D controlled by the QPC gate voltage V_g . Charges emitted by the dot submitted to the excitation $V_{exc}(t)$ are collected through contact 1. (b) Sketch of single-electron emission as described in the text. (c) Modulus of the average current first harmonic $|I_{f_1}|$ in color scale as a function of the excitation amplitude and QPC gate voltage.

of charge e , one can show that $\langle I(t)I(t+t') \rangle = e \langle I(t) \rangle \delta(t')$. If this perfect emission is triggered with period T , we have, after averaging the time t on one drive period, $C_1(t') = \frac{e^2}{T} \delta(t')$. In our case, as one electron and one hole are emitted at each period T , we get for the perfect emitter $C_1(t') = \frac{2e^2}{T} \delta(t')$ with Fourier transform $S_1(\omega) = 4e^2 f_d$. The term $C_2(t')$ can be computed assuming only the exponential relaxation of the average current $\langle I(t) \rangle$, we then get $C_2(t') = \frac{e^2 f_d}{\tau} e^{-|t'|/\tau}$ with Fourier transform given by $S_2(\omega) = \frac{4e^2 f_d}{1 + (\omega\tau)^2}$. Their difference $S(\omega)$ then reads

$$S_{jitter}(\omega) = 4e^2 f_d \times \frac{(\omega\tau)^2}{1 + (\omega\tau)^2}. \quad (1)$$

In this optimum regime, the current fluctuations are not caused by the fluctuations in the number of particles emitted between two triggers but are entirely determined by the quantum uncertainty on the emission time of a single charge. This phase noise, which we call quantum jitter, is the direct illustration that the exponential decay of the average current, which looks like the relaxation of a classical RC circuit, comes from the accumulation of electrons emitted one by one with a random emission time coming from the tunneling process. It can be used as a reference value for perfect on-demand single-particle emission and is fully parametrized by the escape time τ . Equation (1) can thus be experimentally

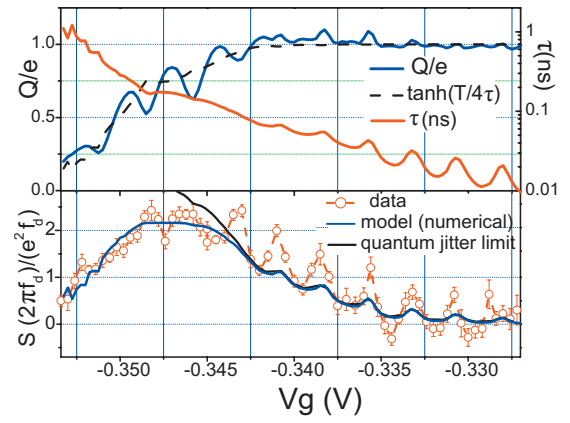


FIG. 2. (Color) (a) Average emitted charge Q and escape time τ for $2eV_{exc} = \Delta$ as a function of V_g . The black dashed line is the $Q(\tau)$ dependence expected for an exponential relaxation: $Q = e \times \tanh \frac{T}{4\tau}$. (b) Experimental current noise spectrum S as a function of V_g for $2eV_{exc} = \Delta$ (red points). The quantum jitter limit $S = 4e^2 f_d \frac{(2\pi f_d \tau)^2}{1 + (2\pi f_d \tau)^2}$, with τ given by the experimental data of figure (a), has been plotted in black. The blue trace corresponds to the predictions of our model.

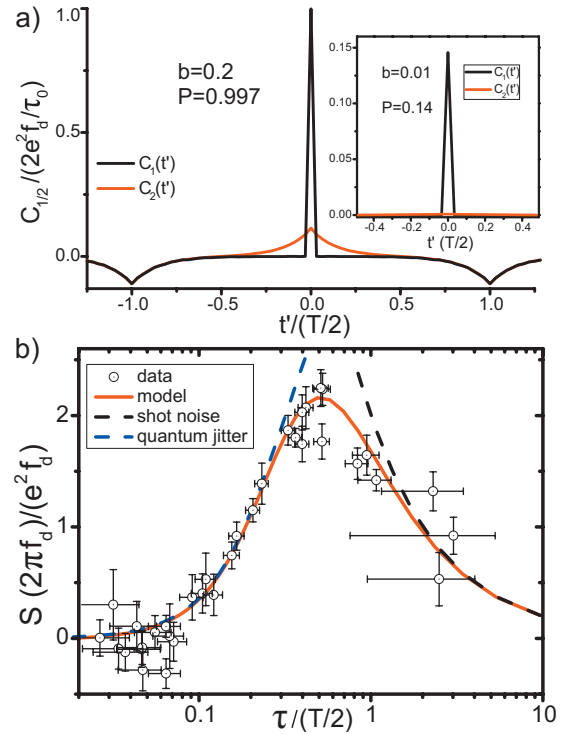


FIG. 3. (Color) (a) Contributions $C_1(t')$ (black) and $C_2(t')$ (red) to the current correlations $C(t')$ in units of $2e^2 f_d / \tau_0$ and as a function of t' for $P=0.997$ ($b=0.2$). Inset: $C_1(t')$ (black) and $C_2(t')$ (red) for $b=0.01$, $P=0.14$. (b) Current noise spectrum $S(2\pi f_d)$ at the center of the diamonds plotted as a function of the average escape time τ . The experimental data are compared to our theoretical predictions without any adjustable parameter. The asymptotic limits of quantum jitter and phase noise are plotted in dashed blue and black lines.

checked by either varying ω at fixed τ or by varying τ at fixed ω . Note that the quantum jittering is encoded in the current correlations on times shorter than the escape time τ or equivalently in the noise spectrum at high frequencies $\omega\tau \approx 1$. To reach subnanosecond time scales relevant for phase-coherent electronics, one needs the use of gigahertz frequencies, in our case, we have $\omega = 2\pi f_d \approx 1/(100 \text{ ps})$.

The short-time behavior of C_1 and C_2 in the opposite limit of long escape time, where the emission probability strongly departs from one, $P \ll 1$ ($b=0.01, P=0.14$), has been plotted in the inset of Fig. 3(a). In that case, the contribution of the average current C_2 is negligible, $C_1 \gg C_2$ and the current spectrum is white (except for very low frequencies) and proportional to P , $S_{\text{shot}}(2\pi f_d) = 4e^2 f_d \times P = e^2 / \tau$. In this $P \ll 1$ limit, single charge emission is a Poissonian random process, the noise reflects these random fluctuations in the emitted charge and usual shot noise is recovered. Between the shot noise and quantum jitter limits, $S(\omega)$ is also fully parametrized by the escape time τ and can be numerically evaluated.¹⁷ An analytic derivation of the noise spectrum in all regimes was even provided in a recent paper.¹⁸

Figure 3(b) represents our current noise data $S(2\pi f_d)$ as a function of τ for operating conditions close to the center of the current diamonds and their comparison with our model. The agreement is excellent within the full range of escape time with no adjustable parameter. In particular, the shot-noise limit $\tau \geq T/2$ and more importantly the quantum jitter limit $\tau \leq T/2$ reproduce *quantitatively* our experimental results. The observation of the quantum jitter limit demonstrates on-demand emission of a single particle without collateral excitations. This corresponds to the optimum operating conditions of the source.

As seen in Fig. 2(b), the model described above accounts quantitatively for all our experimental data except for operating conditions at the edges of the diamonds in the short escape time regime (maxima of the oscillations). At these points, the experimental data systematically fall above the theoretical quantum jitter limit, represented by the black curve. In these operating conditions, the dot charge for the initial and final value of the excitation is not quantized as an energy level is brought at resonance with the Fermi energy. Multiple charge emission then occurs causing an excess of the noise with respect to the quantum jitter limit. These working points cannot be used for single-particle emission.

To conclude, we have measured the high-frequency current autocorrelations of an on-demand single charge emitter. In particular, we have observed the intrinsically high-frequency noise related to the quantum uncertainty on the emission time of single charges. When the noise reduces to this quantum jitter, a single particle is emitted with unit probability between two shots of the source. The use of these correlation techniques on single-electron beams can now be applied to more elaborate electron quantum optics experiments. For example, two electrons interferences have been predicted¹⁹ and observed²⁰ using continuous streams of electrons generated by dc biased ohmic contacts. Here, two electron interferences between single charges emitted on demand could be probed in a Hong-Ou-Mandel-type (Ref. 21) experiment, where two electrons collide on a beam splitter. Perfect antibunching at the beam splitter outputs would reveal the indistinguishability of electrons emitted by two independent sources.^{2,22}

We thank Anne Denis for the fabrication of the 120 Ω impedance matching lines.

*Also at SPEC-CEA Saclay, France.

†feve@lpa.ens.fr

- ¹Y. Ji, Y. Chung, D. Sprinzak, M. Heiblum, D. Mahalu, and H. Shtrikman, *Nature (London)* **422**, 415 (2003).
- ²S. Ol'khovskaya, J. Splettstoesser, M. Moskalets, and M. Büttiker, *Phys. Rev. Lett.* **101**, 166802 (2008).
- ³J. Splettstoesser, M. Moskalets, and M. Büttiker, *Phys. Rev. Lett.* **103**, 076804 (2009).
- ⁴G. Fève *et al.*, *Science* **316**, 1169 (2007).
- ⁵M. D. Blumenthal, B. Kaestner, L. Li, S. Giblin, T. J. B. M. Janssen, M. Pepper, D. Anderson, G. Jones, and D. A. Ritchie, *Nat. Phys.* **3**, 343 (2007).
- ⁶H. le Sueur, C. Altimiras, U. Gennser, A. Cavanna, D. Mailly, and F. Pierre, *Phys. Rev. Lett.* **105**, 056803 (2010); P. Degiovanni, Ch. Grenier, G. Fève, C. Altimiras, H. le Sueur, and F. Pierre, *Phys. Rev. B* **81**, 121302(R) (2010); A. M. Lunde, S. E. Nigg, and M. Büttiker, *ibid.* **81**, 041311(R) (2010).
- ⁷P. Roulleau, F. Portier, P. Roche, A. Cavanna, G. Faini, U. Gennser, and D. Mailly, *Phys. Rev. Lett.* **100**, 126802 (2008).
- ⁸P. Degiovanni, C. Grenier, and G. Fève, *Phys. Rev. B* **80**, 241307(R) (2009).
- ⁹M. Moskalets, P. Samuelsson, and M. Büttiker, *Phys. Rev. Lett.* **100**, 086601 (2008).
- ¹⁰J. Keeling, A. V. Shytov, and L. S. Levitov, *Phys. Rev. Lett.* **101**, 196404 (2008).

- ¹¹M. Vanević, Y. V. Nazarov, and W. Belzig, *Phys. Rev. B* **78**, 245308 (2008).
- ¹²P. Michler *et al.*, *Science* **290**, 2282 (2000); B. Lounis and W. E. Moerner, *Nature (London)* **407**, 491 (2000).
- ¹³A. M. Robinson and V. I. Talyanskii, *Phys. Rev. Lett.* **95**, 247202 (2005); N. Maire, F. Hohls, B. Kaestner, K. Pierz, H. W. Schumacher, and R. J. Haug, *Appl. Phys. Lett.* **92**, 082112 (2008).
- ¹⁴A. Mahé *et al.*, *J. Low Temp. Phys.* **153**, 339 (2008).
- ¹⁵M. Reznikov, M. Heiblum, H. Shtrikman, and D. Mahalu, *Phys. Rev. Lett.* **75**, 3340 (1995); A. Kumar, L. Saminadayar, D. C. Glattli, Y. Jin, and B. Etienne, *ibid.* **76**, 2778 (1996).
- ¹⁶E. Zakka-Bajjani, J. Ségala, F. Portier, P. Roche, D. C. Glattli, A. Cavanna, and Y. Jin, *Phys. Rev. Lett.* **99**, 236803 (2007).
- ¹⁷A. Mahé, Ph.D. thesis, Université Pierre et Marie Curie, 2009.
- ¹⁸M. Albert, C. Flindt, and M. Büttiker, *Phys. Rev. B* **82**, 041407(R) (2010).
- ¹⁹P. Samuelsson, E. V. Sukhorukov, and M. Büttiker, *Phys. Rev. Lett.* **92**, 026805 (2004).
- ²⁰I. Neder *et al.*, *Nature (London)* **448**, 333 (2007).
- ²¹C. K. Hong, Z. Y. Ou, and L. Mandel, *Phys. Rev. Lett.* **59**, 2044 (1987).
- ²²G. Fève, P. Degiovanni, and Th. Jolicœur, *Phys. Rev. B* **77**, 035308 (2008).